Saudi Dental Journal (2020) 32, 396–402

King Saud University

Saudi Dental Journal

www.ksu.edu.sa
www.sciencedirect.com

ORIGINAL ARTICLE

Quantitative and qualitative assessments of intraosseous neurovascular canals in dentate and posteriorly edentulous individuals in lateral maxillary sinus wall

Mohd Yusmiaidil Putera Mohd Yusof [a,b,*], **Michelle Clare Mah** [c], **Nor Hidayah Reduwan** [a], **Kornkamol Kretapirom** [d], **Nur Hafizah Kamar Affendi** [e]

[a] *Centre for Oral & Maxillofacial Diagnostics and Medicine Studies, Faculty of Dentistry, Universiti Teknologi MARA Selangor, Sungai Buloh Campus, 47000 Sungai Buloh, Selangor, Malaysia*
[b] *Institute of Pathology, Laboratory and Forensic Medicine (I-PPerForM), Universiti Teknologi MARA Selangor, Sungai Buloh Campus, 47000 Sungai Buloh, Selangor, Malaysia*
[c] *Centre for Oral & Maxillofacial Surgery Studies, Universiti Teknologi MARA Selangor, Sungai Buloh Campus, 47000 Sungai Buloh, Selangor, Malaysia*
[d] *Department of Oral and Maxillofacial Radiology, Faculty of Dentistry, Mahidol University, Bangkok, Thailand*
[e] *Centre for Restorative Dentistry Studies, Faculty of Dentistry, Universiti Teknologi MARA Selangor, Sungai Buloh Campus, 47000 Sungai Buloh, Selangor, Malaysia*

Received 13 May 2019; revised 29 October 2019; accepted 29 October 2019
Available online 13 November 2019

KEYWORDS

Sinus augmentation;
Maxillary sinus;
Cone-beam CT

Abstract *Objective:* Knowledge and evaluation of the blood supply within the maxillary sinus before sinus augmentation are vital to avoid surgical complications. The lateral maxilla is supplied by branches of the posterior superior alveolar artery and infraorbital artery forming intraosseous anastomoses (IA) within the bony lateral antral wall. This study was undertaken to (i) measure mean diameter of IA and its distance from the alveolar ridge within dentate and posteriorly edentulous subjects and, (ii) qualitatively display the relationship of IA throughout its course within the lateral maxillary sinus in cone beam computed tomography (CBCT).

Method: Maxillary CBCT images of two-hundred-and-fifty-seven consecutive patients (163 men, 94 women, mean age 42 years) were analyzed. Samples were later divided into dentate (n = 142)

* Corresponding author at: Centre for Oral & Maxillofacial Diagnostics and Medicine Studies, Faculty of Dentistry, Universiti Teknologi MARA Selangor, Sungai Buloh Campus, 47000 Sungai Buloh, Selangor, Malaysia.
E-mail address: yusmiaidil@uitm.edu.my (M.Y.P.M. Yusof).

Peer review under responsibility of King Saud University.

Production and hosting by Elsevier

https://doi.org/10.1016/j.sdentj.2019.10.010

and posteriorly edentulous (n = 115) jaws. Using both alveolar ridge and tooth location as reference points, the distance and diameter of IA were assessed.

Result: The IA was seen in 63.7% of all sinuses with 68.2% in dentate and 62.4% in edentulous. Mean distance and diameter of IA across the posterior tooth locations were 17.9 ± 3.0 mm and 1.4 ± 0.5 mm (dentate) and 15.1 ± 3.0 mm and 1.0 ± 0.5 mm (posteriorly edentulous), respectively. In each sample, there were no significant differences in distance-alveolar ridge and no significant correlations in diameter-tooth location. A statistically significant Pearson coefficient correlation between diameter and distance in dentate state was observed ($r = -0.6$).

Conclusion: This study reveals that dentate maxillary jaws present larger diameters as compared to posteriorly edentulous jaws, although the IA course remains the same. As these canal structures contain neurovascular bundles with diameters that may be large enough to cause clinically substantial complications, a thorough pre-surgical planning is therefore highly advisable.

1. Introduction

Knowledge of the neurovascular supply to the maxillary sinus is critical during maxillary sinus floor elevation with the lateral window approach with respect to vascularization of the maxillary sinus graft and the location of blood supply relative to the site of the required lateral osteotomy. The technique invented by Tatum (Tatum, 1986) and first described by Boyne and James (Boyne and James, 1980) has been utilized widely in pre-prosthetic implant surgeries owing to the preservation of the mucoperiosteal membrane of the intact sinus in patients with residual bone of an insufficient height (Yang et al., 2012). Although the surgical severance of one of the vessels may not lead to a life-threatening event, it may obscure the procedure because of difficulty in visualizing the Schneiderian membrane.

The posterior superior alveolar (PSA), infraorbital, and posterior lateral nasal arteries are the three branches of the maxillary artery that supply the maxillary sinus. The PSA artery provides blood supply to the lining of the antrum, posterior teeth, and the maxillary gingivae and mucoperiosteum via its superficial branches (Zijderveld et al., 2008). The dental branch of this artery runs intraosseously, halfway up the lateral sinus wall, and forms a horizontal anastomosis with the infraorbital artery. These intraosseous anastomoses (IAs) supply the Schneiderian membrane, periosteum, and anterolateral sinus wall (Mardinger et al., 2007; Rosano et al., 2009). The infraorbital artery courses through the infraorbital canal and before emerging from the infraorbital foramen, it gives off one or two branches that course caudally along the anterior antral wall (Traxler et al., 1999).

Several studies described the anatomy of the neurovascular canals in the lateral maxillary sinus wall using cadavers (Kqiku et al., 2013; Rosano et al., 2009; Solar et al., 1999; Traxler et al., 1999), computed tomography (Elian et al., 2005; Guncu et al., 2011; Jung et al., 2011; Kang et al., 2013; Mardinger et al., 2007; Yang et al., 2012), and a combination of both (Ella et al., 2008; Rosano et al., 2011). The aim of the present study was to (i) measure the mean diameter of IA and its distance from the alveolar ridge in dentate and posteriorly edentulous patients and (ii) qualitatively display the associations of IA throughout its course within the lateral maxillary sinus on cone-beam computed tomography (CBCT).

2. Materials and methods

The maxillary CBCT scans of consecutive patients scheduled for oral and maxillofacial surgery were included in this study. All patients were referred for CBCT of the maxilla, for various reasons (e.g., pre-implant assessments or third molar extraction), from October 2016 and November 2017. CBCT scans were obtained using the Kodak CS 9300 3D system (Carestream Health Inc., Rochester, NY, USA), with a voxel size of 250 × 250 × 250 µm, a field of view of 17 × 13.5 cm, an X-ray pulse duration of 30 ms, a peak tube voltage of 70 kVp, and a tube current of 10 mA. All reconstructed images were assessed by independent observers in the axial, sagittal, and coronal planes using the Digital Imaging and Communications in Medicine format. The exclusion criteria were CBCT scans with an inadequate quality or a partial cut of the posterior region of the maxilla and presence of bony lesions or fracture lines altering the course of neurovascular structures. CBCT scans were evaluated using the Kodak Digital image communication software (version 6.12.10.0, Carestream Health Inc., Rochester, NY, USA). The workstation was equipped with a 19-in HP LE1911 LCD display (Hewlett-Packard Company, Palo Alto, CA, USA), with a pixel resolution of 1280 × 1024 by two calibrated reviewers. Re-observations were performed after a minimum interval of 1 week. The intra- (MYPM) and inter-rater agreements (MYPM-KK) were assessed using the weighted Kappa scores.

Samples were divided into dentate and posteriorly edentulous jaws. Using the alveolar ridges and tooth location as reference points, the distance and diameter of IA were assessed. For each sample, only the right or left maxillary sinus was analyzed. Canal courses were measured vertically from the alveolar crest in each sagittal reconstruction (Fig. 1). The antero-posterior (A-P) position of the canal was measured from the lateral nasal wall (Mardinger et al., 2007). All A-P distances were divided into four sectors based on the tooth location: first and second premolars and first and second molars. The canal diameter was measured on the coronal reconstruction and analyzed for the presence of teeth (dentate or posteriorly edentulous) and their location. Anatomical descriptions of the location of the full length of IA on the lateral wall of the maxillary sinus on CBCT were predetermined as follows: located along the axis of the ala-tragus line (Camper's line) in the axial

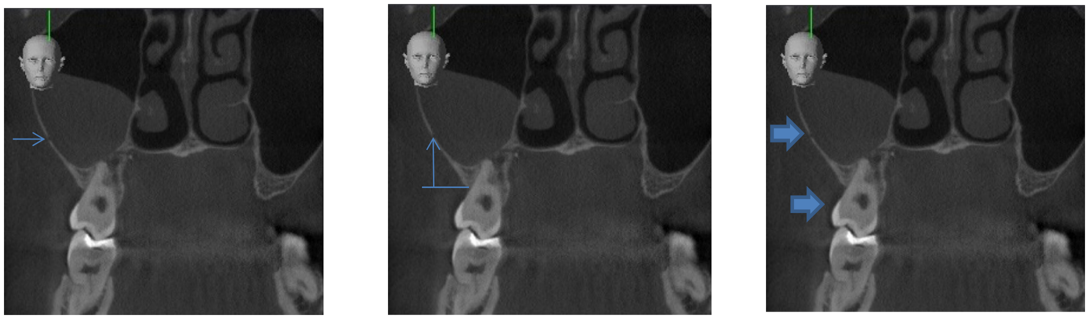

Canal detection | Canal to alveolar ridge distance | Canal diameter according to tooth types

Fig. 1 Detection and measurement of intraosseous anastomosis canal.

view and bounded by the mesiobuccal root or crown of the maxillary first molar (anterior margin), distal surface of the maxillary second molar (posterior margin), and mesiobuccal and mesiopalatal crowns of the maxillary third molar in the coronal view.

All measurements were expressed as mean values and standard deviations. To ensure accurate measurements, CBCT scans were magnified to five times their original size. Differences among the mean distances of all four teeth in the dentate and posteriorly edentulous groups were tested using one-way analysis of variance. If differences among the four points of different teeth were statistically significant, the Bonferroni's method for a post hoc analysis was used. Correlations between the vessel diameter and distance in dentate and posteriorly edentulous groups were tested for statistical significance with the Pearson's correlation test. Statistical significance was set at $p < 0.05$. Analyses were conducted using RStudio software, version 0.97.551 (2009–2012; RStudio, Inc.). The *ggplot2* function was used to develop the graphics in this study.

3. Results

From October 2016 to November 2017, 411 scans utilizing a large field of view (17 × 13.5 cm) were assessed, 37.5% of which were excluded from the study because of the exclusion criteria. The intra- and inter-rater analyses of IA showed weighted Kappa coefficients of 0.94 and 0.78 for the distance, respectively, and 0.87 and 0.71 for the diameter, respectively. The study included 163 men and 94 women, with a mean age of 42 years (range: 23–61 years). There were more fully dentate (n = 142) patients than posteriorly edentulous (n = 115) patients. IA was seen in 63.7% of all sinuses, with 68.2% in dentate patients and 62.4% in posteriorly edentulous patients. The mean distance and diameter of IA from the posterior tooth locations were 17.9 ± 3.0 and 1.4 ± 0.5 mm in dentate and 15.1 ± 3.0 and 1.0 ± 0.5 mm in posteriorly edentulous patients, respectively (Table 1). The mean difference in distance was not significant in the dentate group but was statistically significant in the posteriorly edentulous group (Fig. 2). The first molar region exhibited a significant mean difference compared to all other areas. In dentate patients, the diameter of IA negatively correlated with the distance ($p < 0.05$), whereas there was no statistically significance in either variable in posteriorly edentulous patients (Fig. 3).

Fig. 4 shows the box and whisker plots for the diameter in both dentate and posteriorly edentulous groups based on differences in posterior teeth locations from the first premolar to the second molar. The dentate group exhibited a larger diameter compared to the posteriorly edentulous group. The median values ranged from 1.6 mm to 1.7 mm in dentate patients and 1 mm to 1.2 mm in posteriorly edentulous patients.

4. Discussion

In the present study, IA was detected on CBCT scans in more than 60% of the cases. This was slightly higher than the percentage reported in other published studies, which ranged from 50% (Rysz et al., 2014) to 55% (Elian et al., 2005; Mardinger et al., 2007). A systematic review by Varela-Centelles et al. in 2015 revealed that CBCT detects the PSA artery (78.12%) more frequently than conventional CT (51.19%) and has better sensitivity and cost-effectiveness in the detection of the PSA artery, so it is recommended owing to its lower radiation dosage than conventional CT (Varela-Centelles et al., 2015). Invisible IA in most cases does not exclude its presence, and it could be because of the intrasinusal location and small diameter of the vessel (Ella et al., 2008; Rosano et al., 2009).

Table 1 Distance and diameter of intraosseous anastomosis from tooth location.

Distance (SD) in mm		
Tooth	Dentate	Edentulous
First premolar	19.1 (3.02)	15.5 (2.94)
Second premolar	17.3 (3.11)	15.8 (3.21)
First molar	16.2 (3.12)	11.1 (3.09)
Second molar	16.9 (2.85)	16.8 (3.18)
Mean	17.9 (3.01)	15.1 (3.04)
Diameter (SD) in mm		
First premolar	1.2 (0.5)	0.8 (0.5)
Second premolar	1.3 (0.5)	0.8 (0.5)
First molar	1.4 (0.5)	1.1 (0.5)
Second molar	1.7 (0.5)	1.2 (0.5)
Mean	1.4 (0.5)	1.0 (0.5)

SD standard deviation.

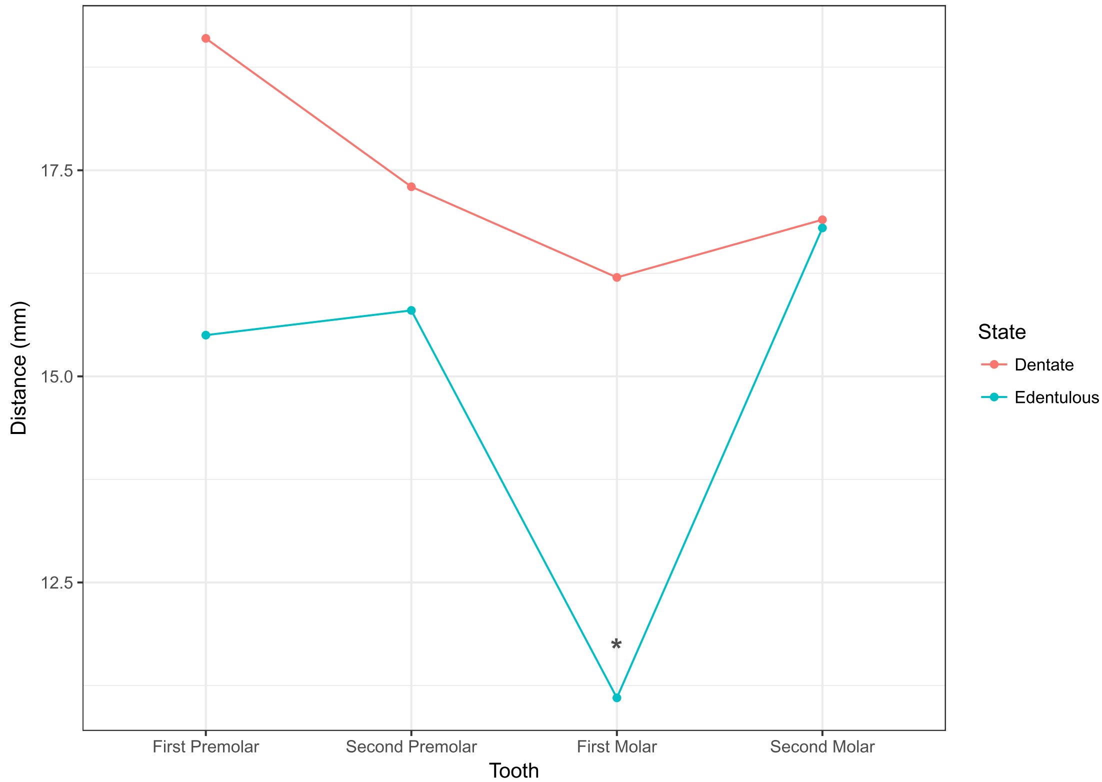

Fig. 2 Mean distance between all teeth areas for dentate and posteriorly edentulous group (*$p < 0.05$).

However, in cases where IA cannot be identified, measurements reported in the present study and similar other studies can be helpful in preventing complications during sinus elevation procedures.

Sinus elevation procedures are mostly performed in the posterior maxilla, except for the maxillary tuberosity region, with an available window height of approximately 13 mm required to place a 10–12-mm implant. The height of the residual ridge is an important parameter to locate the IA vessel and to place implants avoiding the risk of transecting the vessel, especially in cases of severely atrophied ridges. Previous studies reported that the bone window created during a sinus elevation procedure in edentulous patients should not be higher than 15 mm from the alveolar crest (Elian et al., 2005; Mardinger et al., 2007). This requirement was proven in the present study, as the mean distance of IA from the alveolar ridge in edentulous patients was 15.1 ± 3.0 mm. This finding was similar to the finding of a CBCT study by Elian et al. in 2005, in which the distance of IA from the alveolar ridge was approximately 16.4 ± 3.5 mm (in the posterior region of the edentulous maxilla).

As the present study only utilized a specific field of view (17 × 13.5 cm), thereby providing sufficient views for both the left and right maxillary sinuses, further data segregation into dentate and posteriorly edentulous patients was possible. In addition, the number of subjects derived from this segregation was statistically adequate for generalizations. The sample size calculated before the start of the study had revealed the minimum required sample size to be 73. The number of subjects in this study surpassed the required number for both dentate (n = 142) and posteriorly edentulous (n = 115) groups. Nevertheless, the recorded data had slight variations, mostly because of the remaining height of the alveolar ridge, degree of maxillary atrophy in different patients, and influence of tooth position on the determined location of the vessel. These variations were also found in another study (Jensen et al., 1994). This discrepancy could have been caused by different CBCT machines used in different studies. The present study is also the first one assessing the course of IA in dentate and posteriorly edentulous subjects on CBCT with particular specifications. Previous studies evaluated IA of the PSA artery in dentate subjects using human cadavers (Kqiku et al., 2013) and in posteriorly edentulous subjects using CBCT (Yang and Kye, 2014).

Discrepancies also exist in the diameter of the vessels with the potential risk of hemorrhage during surgical procedures. A study by Ulm et al. in 1995 revealed that long-term edentulism caused reduction in the trabecular density and in its connectivity (Ulm et al., 1995). Other authors found that older patients have vessels of a wider diameter. Based on the results of the present study, it is likely that an edentulous patient had vessels of a narrower mean diameter, measuring 1.0 mm, than dentate patients. The vessels with a diameter less than 1 mm may have a lower risk of bleeding during sinus elevation procedures, whereas those with diameter of more than 1.0–2.5 mm may have a higher risk of hemorrhage (Kang et al., 2013; Mardinger et al., 2007). Transecting the vessel may have a drawback of "washing" or pushing the grafting material,

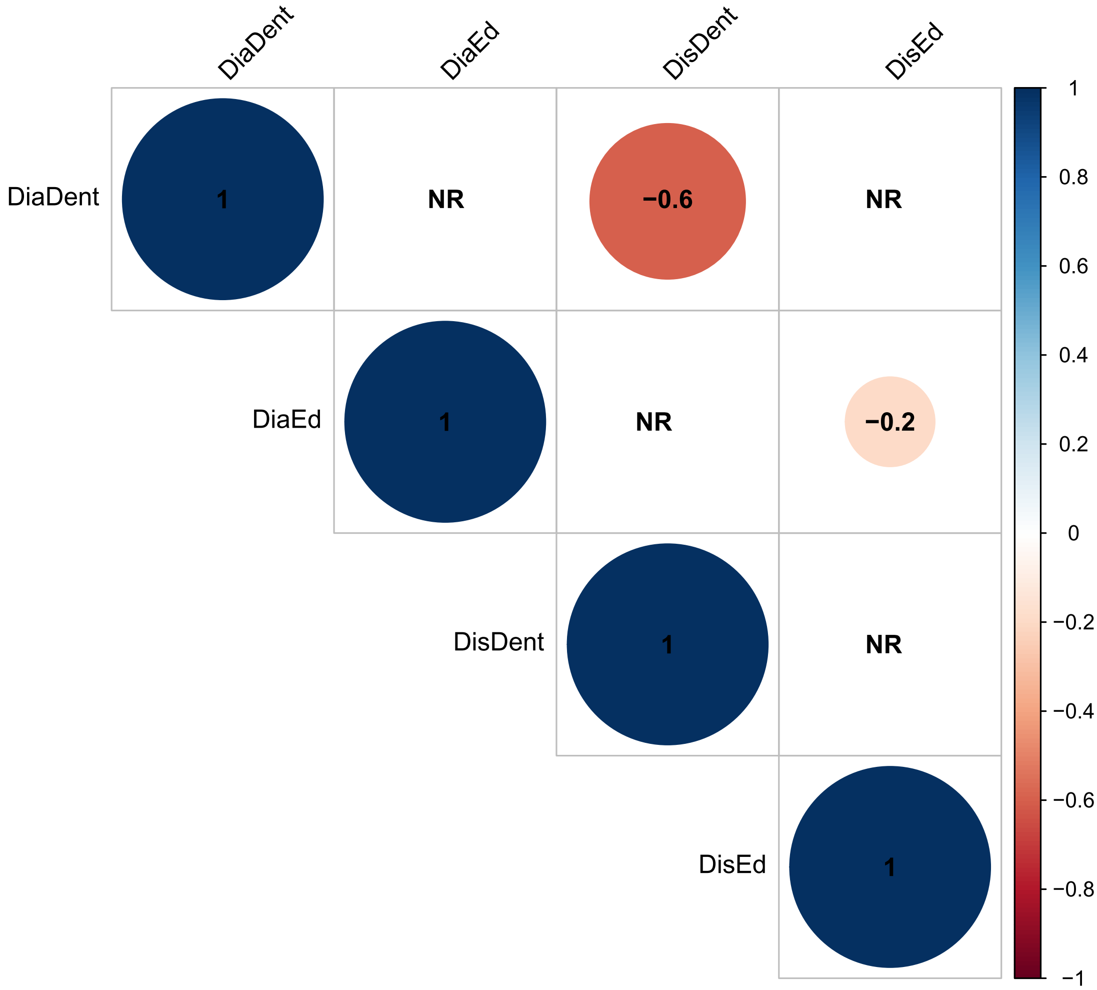

Fig. 3 Correlations between all teeth for dentate and posteriorly edentulous group. DiaDent Diameter in dentate, DiaEd Diameter in edentulous, DisDent Distance in dentate, DisEd Distance in edentulous.

leading to an inadequate fill in ridge augmentation procedures. In addition, profuse bleeding may obscure the view of the surgical field, thus increasing the possibility of Schneiderian membrane perforation (Apostolakis and Bissoon, 2014), which is the most frequently reported intraoperative complication of sinus floor augmentation procedures (Pjetursson et al., 2008). Furthermore, patients are likely to develop postoperative complications, including hematoma of the cheek, sinus mucosal edema, and postoperative sinusitis. The development of sinusitis is expected to occur in sinuses filled with blood or fluid because of the reduced patency of the osteomeatal unit, thereby compromising the ridge augmentation procedure and causing failure to achieve osseointegration (Timmenga et al., 2003).

In addition to the risks of hemorrhage and its complications, vascularization from the arteries that supply the maxillary sinus wall and lining is necessary for good healing and integration of the newly grafted bone during an augmentation procedure, and damage to IA causing impaired vascularization may risk its successful outcome (Boëck-Neto et al., 2009). CBCT performed before the sinus augmentation surgery would allow the operator to carefully consider the location and diameter of the vessel and ridge height and width to preserve the artery and avoid arterial bleeding, especially if the procedure is performed under local anesthesia.

5. Conclusion

This study revealed that the dentate jaws have vessels of larger diameters than posteriorly edentulous jaws. Special precaution should be taken for the first molar region in edentulous jaws as IA tends to be less than 15 mm away from the alveolar ridge. The distance between IA and the alveolar ridge is lesser in edentulous jaws than in dentate jaws. Before surgical sinus elevation and implant placement, information on the available ridge and arterial supply is essential to avoid complications. These data may aid the operator to perform risk assessment and estimate the sinus window design in sinus augmentation procedures. Therefore, based on the results of the present study, a CBCT analysis is essential to detect alterations before the lateral wall approach may be endorsed, and careful attention should be paid in high-risk cases.

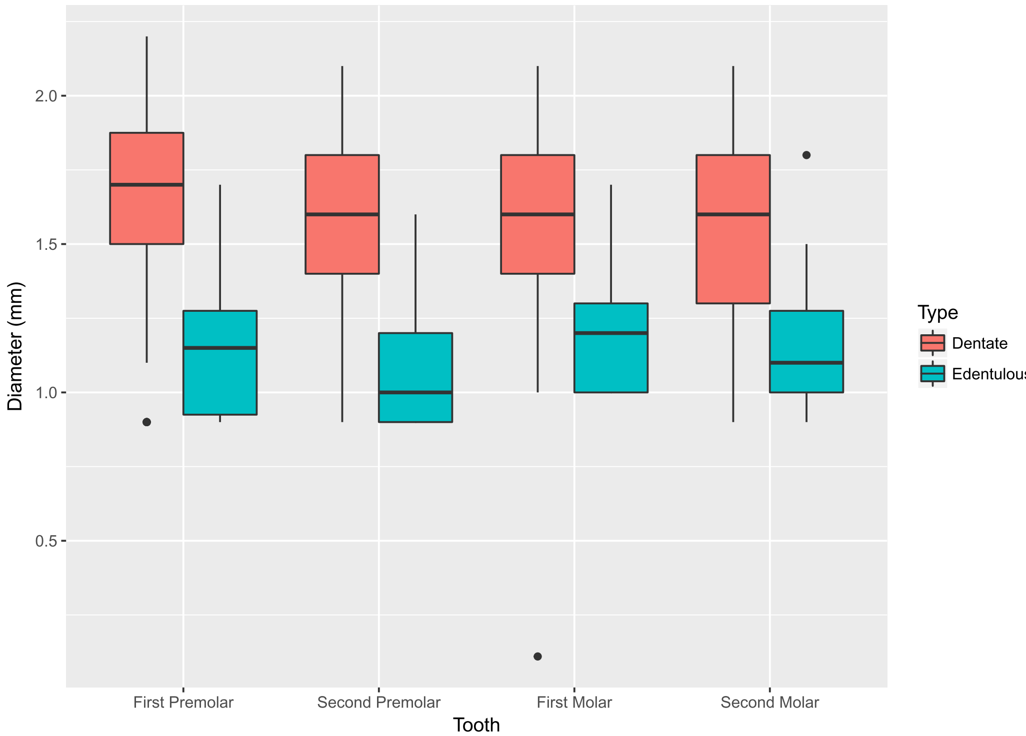

Fig. 4 Box plots for the diameter in both dentate and posteriorly edentulous groups based on different posterior teeth.

Declaration of Competing Interest

The authors declared that there is no conflict of interest.

Acknowledgements

This work was supported by LESTARI Research Grant, Universiti Teknologi MARA Malaysia [600-IRMI 5/3/LESTARI(011/2019)].

References

Apostolakis, D., Bissoon, A.K., 2014. Radiographic evaluation of the superior alveolar canal: measurements of its diameter and of its position in relation to the maxillary sinus floor: a cone beam computerized tomography study. Clin. Oral Implants Res. 25 (5), 553–559.

Boëck-Neto, R.J. et al, 2009. VEGF and MVD expression in sinus augmentation with autologous bone and several graft materials. Oral Dis. 15 (2), 148–154.

Boyne, P.J., James, R.A., 1980. Grafting of the maxillary sinus floor with autogenous marrow and bone. J. Oral Surg. 38 (8), 613–616.

Elian, N., Wallace, S., Cho, S.C., Jalbout, Z.N., Froum, S., 2005. Distribution of the maxillary artery as it relates to sinus floor augmentation. Int. J. Oral Maxillofac. Implants 20 (5), 784–787.

Ella, B. et al, 2008. Vascular connections of the lateral wall of the sinus: surgical effect in sinus augmentation. Int. J. Oral Maxillofac. Implants 23 (6), 1047–1052.

Guncu, G.N., Yildirim, Y.D., Wang, H.L., Tozum, T.F., 2011. Location of posterior superior alveolar artery and evaluation of maxillary sinus anatomy with computerized tomography: a clinical study. Clin. Oral Implants Res. 22 (10), 1164–1167.

Jensen, J., Sindet-Pedersen, S., Oliver, A.J., 1994. Varying treatment strategies for reconstruction of maxillary atrophy with implants: results in 98 patients. J. Oral Maxillofac. Surg. 52 (3), 210–216.

Jung, J., Yim, J.H., Kwon, Y.D., Al-Nawas, B., Kim, G.T., Choi, B.J., Lee, D.W., 2011. A radiographic study of the position and prevalence of the maxillary arterial endosseous anastomosis using cone beam computed tomography. Int. J. Oral Maxillofac. Implants 26 (6), 1273–1278.

Kang, S.J., Shin, S.I., Herr, Y., Kwon, Y.H., Kim, G.T., Chung, J.H., 2013. Anatomical structures in the maxillary sinus related to lateral sinus elevation: a cone beam computed tomographic analysis. Clin. Oral Implants Res. 24, 75–81.

Kqiku, L., Biblekaj, R., Weiglein, A.H., Kqiku, X., Stadtler, P., 2013. Arterial blood architecture of the maxillary sinus in dentate specimens. Croat. Med. J. 54 (2), 180–184.

Mardinger, O., Abba, M., Hirshberg, A., Schwartz-Arad, D., 2007. Prevalence, diameter and course of the maxillary intraosseous vascular canal with relation to sinus augmentation procedure: a radiographic study. Int. J. Oral Maxillofac. Surg. 36 (8), 735–738.

Pjetursson, B.E., Tan, W.C., Zwahlen, M., Lang, N.P., 2008. A systematic review of the success of sinus floor elevation and survival of implants inserted in combination with sinus floor elevation. J. Clin. Periodontol. 35, 216–240.

Rosano, G., Taschieri, S., Gaudy, J.F., Del Fabbro, M., 2009. Maxillary sinus vascularization: a cadaveric study. J. Craniofac. Surg. 20 (3), 940–943.

Rosano, G., Taschieri, S., Gaudy, J.F., Weinstein, T., Del Fabbro, M., 2011. Maxillary sinus vascular anatomy and its relation to sinus lift surgery. Clin. Oral Implants Res. 22 (7), 711–715.

Rysz, M., Ciszek, B., Rogowska, M., Krajewski, R., 2014. Arteries of the anterior wall of the maxilla in sinus lift surgery. Int. J. Oral Maxillofac. Surg. 43 (9), 1127–1130.

Solar, P., Geyerhofer, U., Traxler, H., Windisch, A., Ulm, C., Watzek, G., 1999. Blood supply to the maxillary sinus relevant to sinus floor elevation procedures. Clin. Oral Implants Res. 10 (1), 34–44.

Tatum Jr., H., 1986. Maxillary and sinus implant reconstructions. Dent. Clin. North Am. 30 (2), 207–229.

Timmenga, N.M., Raghoebar, G.M., Liem, R.S., Van Weissenbruch, R., Manson, W.L., Vissink, A., 2003. Effects of maxillary sinus floor elevation surgery on maxillary sinus physiology. Eur. J. Oral Sci. 111 (3), 189–197.

Traxler, H., Windisch, A., Geyerhofer, U., Surd, R., Solar, P., Firbas, W., 1999. Arterial blood supply of the maxillary sinus. Clin. Anat. 12 (6), 417–421.

Ulm, C., Solar, P., Gselimann, B., Matejka, M., Watzek, G., 1995. The edentulous maxillary alveolar process in the region of the maxillary sinus—a study of physical dimension. Int. J. Oral Maxillofac. Surg. 24 (4), 279–282.

Varela-Centelles, P., Loira-Gago, M., Seoane-Romero, J.M., Takkouche, B., Monteiro, L., Seoane, J., 2015. Detection of the posterior superior alveolar artery in the lateral sinus wall using computed tomography/cone beam computed tomography: a prevalence meta-analysis study and systematic review. Int. J. Oral Maxillofac. Surg. 44 (11), 1405–1410.

Yang, S.M., Kye, S.B., 2014. Location of maxillary intraosseous vascular anastomosis based on the tooth position and height of the residual alveolar bone: computed tomographic analysis. J. Periodontal Implant Sci. 44 (2), 50–56.

Yang, S.M., Park, S.I., Kye, S.B., Shin, S.Y., 2012. Computed tomographic assessment of maxillary sinus wall thickness in edentulous patients. J. Oral Rehab. 39 (6), 421–428.

Zijderveld, S.A., van den Bergh, J.P., Schulten, E.A., ten Bruggenkate, C.M., 2008. Anatomical and surgical findings and complications in 100 consecutive maxillary sinus floor elevation procedures. J. Oral Maxillofac. Surg. 66 (7), 1426–1438.